



Published in final edited form as:

Neuron. 2009 December 24; 64(6): 885–897. doi:10.1016/j.neuron.2009.11.007.

The Ion Channel ASIC2 is Required for Baroreceptor and Autonomic Control of the Circulation

Yongjun Lu^{1,*}, Xiuying Ma^{1,*†}, Rasna Sabharwal^{1,*}, Vladislav Snitsarev^{1,*†††}, Donald Morgan¹, Kamal Rahmouni¹, Heather A. Drummond^{1,††}, Carol A. Whiteis¹, Vivian Costa¹, Margaret Price¹, Christopher Benson¹, Michael J. Welsh^{1,2,4}, Mark W. Chapleau^{1,3,4,**}, and François M. Abboud^{1,4,**}

¹ Department of Internal Medicine and Cardiovascular Research Center, University of Iowa, Iowa City, IA 52242

² Howard Hughes Medical Institute, University of Iowa, Iowa City, Iowa 52242

³ Department of Veterans Affairs Medical Center, University of Iowa, Iowa City, Iowa 52242

⁴ Department of Molecular Physiology and Biophysics, University of Iowa, Iowa City, Iowa 52242

SUMMARY

Arterial baroreceptors provide a neural sensory input that reflexly regulates the autonomic drive of the circulation. Our goal was to test the hypothesis that a member of the acid sensing ion channel (ASIC) subfamily of the DEG/ENaC superfamily is an important determinant of the arterial baroreceptor reflex. We found that aortic baroreceptor neurons in the nodose ganglia and their terminals express ASIC2. Conscious ASIC2 null mice developed hypertension, had exaggerated sympathetic and depressed parasympathetic control of the circulation, and a decreased gain of the baroreflex, all indicative of an impaired baroreceptor reflex. Multiple measures of baroreceptor activity each suggests that mechanosensitivity is diminished in ASIC2- null mice. The results define ASIC2 as an important determinant of autonomic circulatory control and of baroreceptor sensitivity.

Correspondence should be addressed to: François M. Abboud MD, University of Iowa, Department of Medicine, 616 MRC, Iowa City, IA 52242; phone 391-335-7708; fax 319-335-6969; (francois-abboud@uiowa.edu).

*These authors contributed equally to this work and are listed alphabetically.

**Drs. Chapleau and Abboud contributed equally as senior investigators.

†Present Address: Merck Research Laboratories, Rahway NJ 07065.

††Present Address: Department of Physiology and Biophysics, University of Mississippi Medical Center, Jackson, Mississippi, 39216.

†††Present Address: Department of Biology & Molecular Biology, Montclair State University, Montclair, NJ 07043.

SUPPLEMENTAL DATA

Supplemental Data contains:

I. Supplementary Figures 1–4;

II. Supplementary Table; and

III. Supplementary Methods and Results.

Author Contributions

Y.L. designed primers and performed molecular studies; X.M. performed neural recordings in vivo; R.S. did the telemetry and bilateral carotid occlusion studies; V.S. performed the EP work on isolated neurons; C.W. performed surgical procedures, prepared cultures and analyzed data; D.M. did the studies on electrical stimulation of aortic depressor nerves in the laboratory of K.R.; H.D. contributed to the initial study design; M.P. contributed to concepts and technical approaches; V.C. developed the transgenic mouse; C.B. contributed to concepts and technical approaches; M.J.W. the work was done in collaboration with the Welsh Laboratory; M.W.C. and F.M.A. designed the study, analyzed the data and wrote the paper.

Publisher's Disclaimer: This is a PDF file of an unedited manuscript that has been accepted for publication. As a service to our customers we are providing this early version of the manuscript. The manuscript will undergo copyediting, typesetting, and review of the resulting proof before it is published in its final citable form. Please note that during the production process errors may be discovered which could affect the content, and all legal disclaimers that apply to the journal pertain.

The genetic disruption of ASIC2 recapitulates the pathological dysautonomia seen in heart failure and hypertension and defines a molecular defect that may be relevant to its development.

INTRODUCTION

The arterial baroreceptor reflex which originates in arterial baroreceptors is a key regulator of arterial blood pressure, blood volume, and the neurohumoral control of the circulation^{1,2}. The baroreceptors are sensory nerve endings in the aortic arch and carotid sinuses. Their somata are located in the nodose ganglia and petrosal ganglia, respectively. An increase in blood pressure stretches the baroreceptor nerve endings and triggers afferent signals that are transmitted centrally via the aortic depressor and carotid sinus nerves and modulate the autonomic efferent activity. Activation of these baroreceptor nerves decreases sympathetic nerve activity and increases parasympathetic nerve activity. Thus, the consequences of activation of baroreceptors are a reduction in heart rate, cardiac output, and vascular resistance that buffer the increase in blood pressure. Chronic impairment of the baroreflex results in sustained increases in sympathetic nerve activity with serious pathologic and morbid consequences in cardiovascular disease states such as hypertension, heart failure, myocardial infarction and stroke³⁻⁵.

The molecular mediators of mechanosensitivity of baroreceptors have been elusive⁶⁻¹⁰. The ASIC (acid sensing ion channel) subfamily is a member of the DEG/ENaC family¹¹ that is highly expressed in the mammalian central and peripheral nervous systems¹²⁻¹⁶. Of the four members of the ASIC subfamily, the ASIC2 subunit appears to be required for some mechanosensory processes in peripheral cutaneous and gastrointestinal nerves^{13,16} and it is also the least acid sensitive¹⁷.

Our goal was to test the hypothesis that ASIC2 is an important determinant of the arterial baroreceptor reflex and hence, of the neurohumoral control of the circulation.

RESULTS

ASIC Expression in Nodose Ganglia and Aortic Baroreceptor Terminals

We first determined that ASICs are expressed in mouse nodose ganglia using quantitative RT-PCR (Figure 1a, 1b). There was a predominance of ASIC2b transcript over ASIC1a, 1b, 2a, and 3. Immunofluorescence of ASIC2 protein (Figure 1c, 1d), was present in most nodose neurons and co-localized with ASIC1 and ASIC3 in some but not all neurons (Figure 1e).

Since the sensing of arterial pressure is initiated at the baroreceptor nerve endings it was important to see if ASIC proteins are expressed in the aortic depressor nerve terminals in the aortic arch. Whole mounts of the aortic arch were used for confocal analysis. We found that ASIC1, 2 and 3 were present and co-localized with neurofilament-L antibody in the nerve fibers (Figure 1f) and/or their terminals (Figure 1g).

The generation of ASIC2 null mice was reported previously^{13,16,18,19}. We found that ASIC2 deletion did not alter mRNA expression of ASIC1a, 1b and 3. The results are in Supplementary Figure 2a, b. Western blotting showed no change in ASIC1 and ASIC3 expression in ASIC2 null compared to WT mice (Supplementary Figure 2c), and immunofluorescence of ASIC1 and ASIC3 was preserved in nodose ganglia and aortic depressor nerve ending respectively, while ASIC2 was absent from the nerve ending (Supplementary Figure 2d and 2e).

Cardiovascular Phenotype in ASIC2 Null Mice

To determine the functional importance of ASIC2 in the neural regulation of the circulation we assessed the autonomic cardiovascular control in conscious, freely moving mice. Using radiotelemetry²⁰ we recorded blood pressure, heart rate and locomotor activity and found significant differences between mice with ASIC2 deletion and WT mice (Figure 2, Supplementary Figure 3).

First, ASIC2 null mice had sustained diurnal increases in blood pressure and heart rate (Figure 2). They were hypertensive with average levels of blood pressure and heart rate that were significantly higher over a 24 hour period compared to WT. The higher levels of blood pressure and heart rate were particularly pronounced during the active phase despite a lower level of activity in the null mice (Figure 2).

Second, we contrasted the arterial baroreceptor reflex in the conscious, freely moving state. The baroreceptor reflex causes a decrease in heart rate when there is an increase in blood pressure and vice versa. Therefore we scanned the telemetry data for spontaneous changes in blood pressure and measured the accompanying change in heart rate (Figure 3a). The apparent gain of the reflex is defined as the change in the interbeat interval divided by the change in the blood pressure.^{21, 22} Figure 3b shows that the average baroreceptor reflex gain was 2.3 ms/mmHg for WT and 1.2 for ASIC2 null mice. Our results indicate that in addition to the reduced gain there is a reduced frequency of engagement of the baroreflex in ASIC2 null mice compared to WT (Figure 3c).

Third, we tested for the presence of dysautonomia and sympathovagal imbalance in the conscious awake state. In response to methyl atropine, the increase in heart rate seen in WT mice was abrogated in the ASIC2 null mice indicating a dramatic reduction in parasympathetic control (Figure 3d). In response to propranolol, the decrease in heart rate was over twofold greater in ASIC2 null mice compared to WT indicating an exaggerated sympathetic control of heart rate (Figure 3e). Moreover, in ASIC2 null mice the magnitude of the fall in BP in response to ganglionic blockade with intraperitoneal chlorisondamine was significantly greater than in WT mice (Figure 3f). This fall in blood pressure reflects largely the sympathetic contribution to total vascular resistance confirming that ASIC2 deletion caused an exaggerated sympathetic control of blood pressure and significant dysautonomia.

Thus, the results of the conscious studies in ASIC2 null mice indicate a significant impairment of the baroreflex with consequential increases in arterial blood pressure and heart rate and a sympathovagal imbalance with exaggerated sympathetic and suppressed parasympathetic control.

Since ASICs are expressed in the CNS and in peripheral sensory nerves we wondered whether the impaired baroreflex and the dysautonomia were associated with impaired baroreceptor sensory signaling and whether the central component of the baroreflex was impaired.

Central Mediation of the Baroreflex in ASIC2 Null Mice vs. WT

The central component was examined in anesthetized mice with electrical stimulation of the isolated left aortic depressor nerve with impulses at 10V, 2 msec duration and increasing frequencies of 2.5, 5.0, 10, 20, 30 and 40 Hz for a period of 20 seconds. Reductions in blood pressure and heart rate were seen during the stimulations in both groups and their magnitude increased with the increases in frequency of stimulation (Figure 4). Responses were not different in ASIC2 null mice and wild type (ANOVA—F ratio 0.28 and 0.08 for systolic arterial pressure and heart rate respectively with P values >0.5). The results suggest that the impaired baroreflex and the autonomic dysfunction did not result from a defect in the central mediation of the reflex.

Evidence for Impaired Baroreceptor Sensitivity in ASIC2 Null Mice

To test whether baroreceptor sensitivity was impaired in ASIC2 null mice we used 3 approaches. Baroreceptor activation was tested *in vitro* with measurements of mechanosensitivity of isolated nodose neurons and *in vivo*, with measurements of aortic depressor nerve activity and of pressor responses to bilateral carotid occlusion.

In several *in vitro* studies of mechano-electrical transduction of isolated baroreceptor neurons we reported the effects of graded deformation of the neurons^{23–26}. *In vivo*, the direct measurement of baroreceptor activity from the aortic depressor nerve during phenylephrine-induced hypertension provides a measure of baroreceptor sensitivity in anesthetized mice²⁷. Also, *in vivo*, the magnitude of the reflex increase in blood pressure during bilateral carotid occlusion, which causes a precipitous fall of pressure in the carotid sinuses, reflects the sensitivity of carotid baroreceptors²⁸.

Mechanosensitivity of isolated neurons—In the *in vitro* studies, we first determined mechanosensitivity and ASIC2 expression in aortic baroreceptor neurons vs. non baroreceptor nodose neurons. We anticipated that the aortic baroreceptor neurons might be more mechanosensitive since *in vivo* they continuously sense the changes in pressure with every pulse in contrast to other nodose neurons that innervate parenchymal organs. We identified aortic baroreceptor neurons in the nodose ganglia by labeling them retrogradely with the tracer DiI (1,1' – dioleyl – 3,3,3',3'-tetramethylindocarbocyanine methanesulfonate) injected into the adventitia of the aortic arch as described previously^{9,23,24,29} (Figure 5a). The dispersed neurons in culture were mechanically stimulated with extracellular buffer ejected at 10 psi for 3 s from a micropipette using a pneumatic PicoPump (Figure 5b). The results indicated that the fluorescent aortic baroreceptor neurons were significantly more mechanosensitive generating greater depolarizations than the non-labelled neurons (Figure 5c). Using single-cell RT-PCR we found that ASIC2 mRNA levels in DiI labelled aortic baroreceptor neurons (n=24) from WKY rats were three fold greater than those of non-labelled neurons (n=24) (Figures 5d, 5e).

To further test the influence of ASIC2 expression on mechanosensitivity we compared the mechanically-induced depolarization of isolated nodose neurons from transgenic (Tg) mice overexpressing ASIC2a to those from WT and from ASIC2 null mice. Figure 6 shows a significant degree of variability between individual neurons in each group presumably because the different neurons of the nodose ganglia have sensory terminals in diverse visceral organs and thus variable degrees of mechanosensitivity. However, the percentage of neurons that depolarized more than 1.0 mV was 86% in Tg (n=14), 63% in WT (n=24), and 26% in null mice (n=23). Corresponding depolarizations were significantly different between the three groups averaging 11.24 ± 2.20 mV; 2.73 ± 0.67 mV and 0.86 ± 0.53 mV respectively (Figure 6). Furthermore, in most Tg neurons the depolarizations were sustained for 10 to 20 seconds after the end of mechanical stimulation with a prolonged time constant ($\tau = 7.52 \pm 1.53$ sec, n=12). The depolarizations in WT and KO neurons were rarely sustained more than 3 to 5 seconds (Figure 6).

Aortic depressor nerve activity—We then tested whether impaired mechanosensitivity of baroreceptors in ASIC2 null mice would be detected *in vivo* by measuring aortic depressor nerve activity (ADN) during a rise in arterial pressure. Under pentobarbital anesthesia, the baseline blood pressure and the aortic depressor nerve activity were similar in ASIC2 null and WT mice (Figure 7a). During the decrease in blood pressure with intravenous sodium nitroprusside (SNP), nerve activity was reduced to a low level in both WT and ASIC2 null mice. In response to the rapid initial increase in pressure with phenylephrine (PE) the activity measured as spike frequency and integrated voltage, rose abruptly to a comparable peak level

in both groups within 5 seconds. The nerve activity then declined and stabilized while arterial pressure reached a plateau within the subsequent 10–25 seconds. Although the increase in pressure tended to be higher in the ASIC2 null mice, the decline in ADN activity was steeper reaching the plateau phase at a significantly lower level than in WT mice (Figure 7b). Thus deletion of ASIC2 did not suppress the onset but did suppress the maintenance of nerve activity. Both the increase in frequency of action potentials per mmHg increase in arterial pressure from control, as well as the increase in integrated voltage from control, were more than halved in ASIC2 null mice (Figure 7c).

Bilateral carotid occlusion—Finally, we tested whether the blunted baroreceptor activity of both the aortic and carotid baroreceptors in ASIC2 null mice results in a reduced baroreceptor reflex and may therefore account for the dysautonomia. Bilateral carotid occlusion causes a rapid drop in blood pressure restricted to the carotid circulation and the carotid sinuses and triggers a reflex rise in systemic blood pressure (Figure 8a). The magnitude of the reflex rise in pressure reflects the decrease in carotid baroreceptor nerve activity during the occlusion and the opposing (buffering) effect of the increased aortic baroreceptor activity that occurs during the rise in systemic arterial pressure. In contrasting the carotid occlusion reflex before and after aortic baroreceptor denervation, by sectioning both the right and left aortic depressor nerves (ADNs), we were able to define the magnitude of the buffering effect of the ADN activity on the pressor response. We found that before section of ADNs, the carotid occlusion pressor response was comparable in the KO and WT (Figure 8b). However, after section of ADNs the reflex was significantly enhanced in WT mice and unchanged in the ASIC2 null mice (Figure 8b). This indicates that the ADN activity during the reflex rise in pressure with carotid occlusion was significantly higher in WT compared to KO mice causing an effective buffering and suppression of the reflex that is removed with section of the ADNs. In contrast, the already blunted activation of ADNs during carotid occlusion in ASIC2 null mice prevented a significant augmentation of the pressor response to carotid occlusion after section of the ADNs. Also, the significantly attenuated pressor response in ASIC2 null mice vs. WT after section of ADNs most likely reflects a suppressed baseline carotid baroreceptor afferent activity (Figure 8b).

DISCUSSION

Our data provide the first evidence of a significant contribution of ASIC2 to the neurohumoral regulation of the circulation and to the activation of arterial baroreceptors. Sensory neural signals generated at the baroreceptor are major determinants of sympathetic and parasympathetic nerve activity. In humans with cardiovascular diseases, a dysautonomic state of increased sympathetic nerve activity, decreased parasympathetic nerve activity, and decreased baroreflex sensitivity predict a higher mortality in hypertension, heart failure, diabetes, myocardial infarction and stroke^{3–5,30,31}. Our finding that disrupting the *ASIC2* gene replicates this dysautonomic state and impairs baroreceptor signaling provides an important step in understanding a major pathophysiological process at a molecular level.

In animal models of heart failure and myocardial infarction, chronic electrical activation of the baroreceptors³² or chronic vagal nerve stimulation³³ markedly improves survival. Of additional clinical relevance is the fact that activation of baroreceptor reflexes by electrical stimulation of carotid sinus nerves has been used in humans to treat chronic recurring angina in the 1960s³⁴ and is currently the subject of a clinical trial for the treatment of drug-resistant hypertension with encouraging preliminary results³⁵.

Molecular identification of ion channels in baroreceptors

Following the discovery of stretch-activated ion channels by Guharay and Sachs in chick-embryo skeletal muscle⁶, we explored the possibility that similar channels are involved in

mechano-electrical transduction of baroreceptor nerve activity. Our rationale was twofold. One was the exquisite sensitivity of baroreceptor nerves to the mechanical stimulus of vascular stretch during the arterial pressure pulse, and second was the serious pathologic implication of a loss of the baroreceptor sensitivity³⁻⁵ (see also legend to Supplementary Figure 1). Thus we published our first observation proposing the similarity between the S-A channels in chick-embryo and the baroreceptor nerve activity based on their selective pharmacologic blockade with gadolinium⁸. This was followed by our characterization of mechanically induced inward current, depolarization, and increase in cytosolic calcium in isolated aortic baroreceptor neurons²³⁻²⁶.

The molecular identity of ion channels involved in mechanotransduction had remained obscure however until the genetic studies of Chalfie, Driscoll and their collaborators, who identified in *C. Elegans* eukaryotic genes that encode channels responsible for the transduction of touch, proprioception and locomotor activity³⁶⁻³⁸. A sequence identity between the nematode mechanotransducing genes and the mammalian epithelial Na⁺ channels (ENaC) helped define the degenerin/epithelial Na channel (DEG/ENaC) superfamily of ion channels^{7, 39, 40}.

Our results⁹ were the first demonstration that members of the DEG/ENaC super family are important molecular components of the mechano-electrical transducer complex in arterial baroreceptors. We found that transcripts of the β and γ subunits of ENaC were expressed in nodose neurons and that the γ subunit was localized at the site of mechanotransduction in baroreceptor nerve terminals innervating the aortic and carotic sinuses of rat.⁹ We also found inhibition of responses of isolated aortic baroreceptor neurons to mechanical stimulation by amiloride, and blockade of baroreceptor nerve activity and baroreflex control of blood pressure by the amiloride analog benzamil.⁹ Because the α subunit of ENaC was not expressed, we proposed that the epithelial Na⁺ channel itself is not the mechanosensor, but it was more likely that other, as yet unidentified subunits, multimerize with γ and possibly β subunits to form a membrane complex that interacts with cytoskeletal and matrix proteins to form the mechanosensor.

Following the subsequent discovery by Price et al.¹³ in 2000 that the brain sodium channel BNC1 (ASIC2 by current classification) contributes to touch sensitivity and the findings that it is localized in peripheral mechanosensory terminals of dorsal root ganglia neurons¹⁴, we tested its role in mechanotransduction of arterial baroreceptors. We report here that ASIC2 disruption results in severe dysregulation of neurohumoral control of the circulation, replicates the dysautonomia seen in human hypertension and heart failure and impairs baroreceptor mechanosensitivity. The finding provides a rationale for exploration of defective expression of ASIC2 in these disease states, and evidence to support the use of electrical stimulation of the carotid baroreceptors as a potential therapeutic intervention for patients with intractable drug-resistant hypertension³⁵ and possibly for the exaggerated neurohumoral drive in chronic heart failure.

Contributions of Other Ion Channel Subunits to Baroreceptor Activity

There is evidence that other members of evolutionary conserved ion channel families may contribute to mechanosensitivity of baroreceptors. ENaCs for example may function as mechanosensors in a variety of cell types^{9, 41-43}. Transient receptor potential (TRP) channels that represent another superfamily of cation-selective channels,⁴⁴ are very weakly voltage dependent, are implicated in a variety of sensory transduction processes including mechanosensation,⁴⁵ and are expressed in sensory neurons in rat nodose ganglia and nerve terminals in aortic arch⁴⁶. Their responsiveness to both mechanical and chemical stimuli suggests that they may modulate mechanosensitivity both directly and indirectly through their sensitivity to G protein-coupled receptor activation and second messengers⁴⁷.

In addition to ASIC2, the other ASIC subunits 1 and 3 that are co-expressed in nodose neurons and specifically in the aortic baroreceptor nerve terminals may form a heteromultimeric ASIC channel with ASIC2 and contribute to mechanosensitivity, especially after deletion of ASIC2. In preliminary experiments we noted that the additional deletion of ASIC1 and 3 in the ASIC2 null mice eliminated a significant portion of the remaining pressor response to bilateral carotid occlusion (unpublished observations). In fact ASIC1, 2 and 3 have been shown to contribute differentially to mechanotransduction in different types of gastrointestinal afferents^{16,48}. Their contribution varies depending on the type of neuron and nature of the mechanical stimulus.

The formation of a mechanosensitive channel complex likely involves multiple proteins. In addition to heteromultimers of ASIC subunits, the complex might involve subunits from different families.⁴⁹ A recent report indicates that a heteromeric assembly of ASIC and ENaC subunits may occur in a variety of cell types where they are co-expressed and account for the diversity of amiloride sensitive conductances observed in different tissues⁵⁰. Moreover mechano-electrical transduction depends on accessory tethering proteins such as stomatin and PICK1 that link the channel to the cytoskeleton and extracellular matrix^{51–53}.

Link between baroreceptor nerve activity and the baroreflex autonomic control

Mechanical stimulation of aortic and carotid baroreceptors during a rise in arterial pressure results in reflex activation of parasympathetic drive reducing heart rate, and inhibition of sympathetic nerve activity thereby buffering the rise in arterial pressure. In these experiments we show that in the ASIC2 null mice the mechanosensitivity of baroreceptors is impaired. We also show evidence of reduced parasympathetic control of heart rate, enhanced sympathetic control of both heart rate and vascular resistance and a dysautonomia associated with hypertension. We believe our findings with bilateral carotid occlusion before and after denervation of aortic baroreceptors, establish a link between the reduced baroreceptor signaling of both aortic and carotid baroreceptors in ASIC2 null mice and the significant impairment of the baroreflex control of arterial pressure and heart rate in the dysautonomic phenotype. Moreover, the preserved reflex bradycardia and hypotension during electrical stimulation of the aortic depressor nerve in ASIC2 null mice excludes a contribution of the central component of the reflex and confirms the role of the impaired baroreceptor afferent signaling.

In previous studies from our laboratory we established a significant link between the magnitude of baroreceptor input from the two sets of arterial baroreceptors, the aortic and carotid, and the reflex autonomic control of heart rate and sympathetic nerve activity^{54–56}. We reported that denervation of only one set of either the aortic or carotid nerves reduced significantly the reflex activation of the parasympathetic nerves and the reflex bradycardia without altering the reflex sympatho-inhibition in response to phenylephrine infusion; and the additional denervation of the second set of baroreceptors prevented the reflex sympatho-inhibition.⁵⁴ In rabbits with renal hypertension the baroreflex control of heart rate is impaired, reflecting the known reduction in baroreceptor sensitivity. In these hypertensive rabbits the denervation of only one set of baroreceptors attenuated the reflex inhibition of sympathetic nerve.⁵⁵ Moreover, the electrical stimulation of the aortic depressor nerves in these hypertensive rabbits caused a significant reduction in heart rate and sympathetic nerve activity supporting the notion that the impaired autonomic control and exaggerated sympathetic drive in hypertension resulted from the reduced baroreceptor signaling and not from a central impairment of reflex sympatho-inhibition. Only in severe and prolonged hypertension did we notice some reduction in the central mediation of the baroreflex.⁵⁶ These experiments established a link between the sequential reduction of baroreceptor signaling and a progressive impairment of the autonomic control of heart rate and sympathetic nerve activity.

Conclusion

We conclude that despite the complexity of mechanotransduction and its diversity in different sensory terminals, our results support an important role of ASIC2 in maintaining the integrity of the arterial baroreceptor reflex and the sensitivity of the baroreceptor neurons. Although after its disruption other channels may maintain a residual level of baroreceptor sensitivity, the resulting dysautonomia recapitulates to a significant degree what is seen in cardiovascular diseases where an impairment of the baroreceptor reflex represents a high risk for increased mortality.

EXPERIMENTAL PROCEDURES

All experimental protocols have been approved by the University of Iowa Animal Care Committee in conformance to regulatory standards established by the Association for Assessment and Accreditation of Laboratory Animal Care International (AAALAC). More details about Methods are provided in the supplement. The majority of the methods have been published.

ASIC Expression in Nodose Ganglia Neurons and Aortic Baroreceptor Terminals

Reverse Transcription PCR was used to detect mRNA expression of ASICs in ganglia of rodents¹³. Similarly, Western blots of the ganglia and immunohistochemistry of nodose neurons and their baroreceptor terminals in the aortic arch were reported^{9,13}. Total tissue RNA, extracted with the RNeasy mini kit (Qiagen) from the nodose ganglia, was reverse transcribed into cDNA by using Omniscript RT Kit (Qiagen) and the target sequence was amplified by using the reagent platinum PCR superMix (Invitrogen) and the same PCR program as used in the genotyping.

Quantitative RT-PCR (MX3000P system) was used with Brilliant SYBR Green QPCR Master Mix (Stratagene) and primers were designed in our laboratory and purchased from IDT (Integrated DNA Technologies – Iowa), targeting mouse or rat ASIC1a, ASIC1b, ASIC2a, ASIC2b, and ASIC3 mRNAs, as shown in Table 1, p. 14 in Supplementary Information. The $\Delta\Delta C_T$ method was applied for the data analysis. In order to calculate the copy numbers of target mRNAs of different genes we used Maxiscript SP6/T7 kit (Ambion) to synthesize the standard RNAs from the target cDNA templates, and the serial diluted standard RNAs of known concentrations were subjected to reverse transcription and PCR. This allowed a relative estimate of various ASICs mRNA.

For single cell quantitative RT-PCR of ASIC2, individual neurons cultured on 2.5 cm coverslip were aspirated into a glass microcapillary tube (10–15 μm). The selected cells were transferred into 5 μl of RT solution (kit from Stratagene), and stored at -20°C . When ready for extraction, the cells were incubated at 45°C for 3 min, and vortexed twice (each for 15 s) to release the mRNA. The same RT-PCR program referred to was run. We used GAPDH for normalization of ASIC2 results. In the $\Delta\Delta C_T$ method for single cell qPCR, expression is based on the threshold cycles (C_T). The less expression, the larger C_T values. The C_T values for ASIC2a is 33.8 ± 2.0 cycles and for GAPDH it is 21.3 ± 0.5 cycles, which means that the expression of GAPDH is much higher than ASIC2a. The expression had been normalized and converted into relative mRNA expression in our analysis.

For Western blots, ten nodose ganglia obtained from 5 mice as above were pooled, washed twice with PBS, and homogenized in lysis buffer. Proteins (60 μg) were run on a SDS-7.5% Tris-HCl polyacrylamide gel, and then transferred electrophoretically to a nitrocellulose membrane for detection of chemiluminescence (Pierce Chemical). Goat anti-ASIC antibody

(1:200, Santa Cruz) and horseradish peroxidase- conjugated donkey anti-goat IgG (1:2,000, Santa Cruz) were used.

For the immunohistochemistry of baroreceptor terminals, frozen sections of 10 μm and whole mounts of aortic arches were examined under confocal microscopy (Bio-Rad 1024) equipped with Argon lasers (488 and 514 nm) and helium-neon (543 nm), and the images were analyzed with ImageJ software. Antibodies (Santa Cruz) were used for single- or double-labeling. TSAFS (Tyramide Signal Amplification plus Fluorescence System, Perkin Elmer) was used for enhancement of the double-labeling of ASICs and NNF-L, and intermediate neurofilament.

Gene Deletion of ASIC2 and Transgenic Expression in Mice

The generation of ASIC2 null mice has been reported previously^{13,16,18,19}. Briefly, the sequence encoding the second transmembrane domain (TM2) of ASIC2 protein which is similar in ASIC2a and 2b, was replaced with the vector containing the loxP-PGK sequence and a neomycin resistance cassette. Extract-N-Amp Tissue PCR kit (Sigma) with the gene specific primers was used for genotyping by amplifying tail DNA with designed primers purchased from IDT (Iowa City).

Experiments on awake and anesthetized mice were done either on congenic ASIC2 null mice and C57 BL/6 control mice (telemetry, bilateral carotid occlusion and ADN stimulations) or on ASIC2 null and littermate control mice generated from mixed background (C57BL/6 and 129SVJ) heterozygote mating pairs (measurements of ADN activity).

For the generation of ASIC2a transgenic mice we expressed ASIC2a with five repeats of the c-myc epitope tag inserted at the N-terminus using the same method and vector (containing the pan-neuronal synapsin I promoter) in C57BL/6 and SJL as previously described.⁵⁷

Radiotelemetry Recording of Blood Pressure, Heart Rate and Locomotor Activity in Conscious Mice

The continuous recording of blood pressure and heart rate by telemetry in conscious rodents has been established²⁰. It allowed the assessment of sympathetic and parasympathetic drive to the circulation, the gain of the baroreceptor reflex in the awake state,^{21,22} and the definition of the cardiovascular phenotype of the ASIC2 null mice. (See Supplementary Figure 3)

Under anesthesia, the blood pressure probe (TA11PA-C10, DSI, USA) was inserted into the left carotid artery caudal to the carotid bifurcation and advanced to place the pressure-sensing catheter tip in the aorta. At least 5 days after recovery, diurnal changes in blood pressure, heart rate and locomotor activity were measured in the conscious freely moving state, over a minimum of 24 hrs at a sampling rate of 500Hz for 10 sec periods every 5 min (Dataquest ART Acquisition 4.0, DSI, USA).

The baroreflex sensitivity was estimated from spontaneous reciprocal fluctuations in blood pressure and heart rate using the sequence technique and a custom-made software (Hemolab 2.3, University of Iowa, USA)^{21,22}. Recordings were obtained at a high sampling rate of 2000 Hz over a period of 60 minutes. The number of pulse sequences where changes in systolic blood pressure and pulse interval (PI) correlated positively ($r^2 > 0.85$) for four consecutive beats or more were counted. The average ratio of the systolic BP-PI sequences ($\Delta\text{ms}/\Delta\text{mmHg}$) provided a measure of the baroreceptor gain or sensitivity. The number of baroreceptor sequences per 1000 heart beats provided an index of the extent of engagement of the reflex.

Electrical Stimulation of Aortic Depressor Nerves

We previously reported the experimental protocol.²⁷ Mice weighing 20–30 gms were anesthetized with ketamine (91 µg/g ip) and xylazine (9.1 µg/g ip). Supplemental doses of anesthetics were administered intravenously as needed to prevent eye blink, withdrawal reflexes and fluctuations in arterial blood pressure. Body temperature was maintained at 37.5 °C with a temperature-controlled surgical table and lamp. A cervical midline incision was performed and the trachea was cannulated with polyethylene tubing (PE-50) to facilitate ventilation in an oxygen-enriched chamber for the spontaneously breathing mice. Next, the left femoral artery and the right jugular vein were cannulated with micro-renalthane tubing (MRE 040). Arterial pressure was measured from the left femoral artery with a pressure transducer (BP-100) and heart rate was simultaneously derived from the femoral arterial pressure pulse. Signals were routed to a MacLab data acquisition system (MacLab 8s) for data analysis and storage.

The left aortic depressor nerve was identified in the cervical region using a dissecting microscope and the nerve was isolated from surrounding connective tissue and placed on a bipolar platinum electrode. The nerve was crushed at a point caudal to the electrode. The nerve was stimulated with rectangular pulses of 10-V, 2-ms duration that were delivered to the electrode at 2.5, 5, 10, 20, 30, and 40 Hz from a stimulator (Grass, model S48) for a period of 20 sec.

Mechanical Responses of Isolated Nodose Neurons

Neurons from nodose ganglia were isolated and cultured as previously described^{23–26}. Aortic baroreceptor nodose neurons were labeled by application of the lipophilic fluorescent dicarbocyanine dye DiI (Molecular Probes, OR) into the adventitia of the aortic arch (2 µl of 50 mg/ml solution) as described previously^{24,26,29} and identified by using Rhodamine filter set on the stage of Diaphot TMD microscope (Nikon).

Sharp microelectrodes (100–250 MΩ) were pulled with a P-2000 puller (Sutter, Novato, CA, USA) and filled with KCl (1 M) solution and inserted into the neurons. Under the current clamp mode we measured the depolarizations and action potential generation in response to mechanical stimuli. Records were obtained and analyzed using Axoprobe-1A and Clampex 8 software and Clampfit 8 (Axon Instruments, Union City, CA, USA), and plotted with Origin 7 software (OriginLab Corp., Northampton, MA, USA).

Mechanical deformation was elicited with extracellular buffer ejected at various pressures with a pneumatic PicoPump (Model PV830) (WPI, Sarasota, FL, USA) through a pipette (2 µm in diameter) with its tip placed 10 µm from the cell surface. In earlier studies²⁴ (*portrayed in the Supplemental Data Figure 4*) we showed that the graded ejection pressures caused progressive deformations of the neurons and induced parallel incremental Ca²⁺ transients. These studies showed that at 5, 10, or 15 psi pressure, the ejections caused progressive increases in intracellular calcium which coincided with linear increases in neuronal deformation.

Measurements of Aortic Depressor Nerve (ADN) Activity in Anesthetized Mice

The mice were anesthetized with sodium pentobarbital (60 g/g, ip) with supplemental doses as deemed necessary. The left ADN was identified in the cervical region using a dissecting microscope as previously described²⁷. It was placed on miniaturized bipolar platinum electrodes (0.12 mm outer diameter) and encased in Wacker silicone gel (Adrian, MI). Nerve activity was amplified using a high-impedance probe and a Grass band-pass amplifier (HIP 511J, Grass Instrument Co., Quincy, MA; the low and high frequency cut-off 0.03–3 kHz). The neurogram was displayed on a dual-beam storage oscilloscope (Tektronix 5113, Beaverton, OR) and listened to through an audio speaker.

Aortic baroreceptor sensitivity was evaluated by calculating ADN activity during changes in blood pressure induced by intravenous injection of sodium nitroprusside (SNP) (0.5–2 g/g) followed by phenylephrine (PE) (5–20 g/g). Group comparisons of data obtained following PE included: the increase from baseline control values in the number of spikes · sec per mm Hg increase in blood pressure, and the corresponding increase in integrated voltage expressed as % of maximum voltage.

Responses to Bilateral Carotid Artery Occlusion Before and After Section of Aortic Depressor Nerves

In anesthetized mice (sodium pentobarbital 60 mg/g ip), the systemic arterial pressure was recorded before, during and after a 30 sec period of bilateral carotid occlusion in mice both before and after bilateral section of the aortic depressor nerves. Before bilateral carotid occlusion, baseline arterial pressure was not statistically higher in the null mice than in WT as reported by telemetry in the conscious freely moving state. The difference in arterial pressure between the two groups is minimized under pentobarbital anesthesia.

The increase in arterial pressure with bilateral carotid occlusion is a result of the reflex increase in sympathetic nerve activity triggered by the precipitous drop in carotid sinus pressure and in carotid baroreceptor nerve activity. This pressor response is modulated by the buffering influence of the ADNs that are simultaneously activated during the rise in systemic arterial pressure. The contribution of the latter response is determined by section of the ADNs. The responses to carotid occlusion following section of the ADNs represent the contribution of the carotid baroreceptors.

For an optimal assessment of sensitivity of carotid baroreceptors during bilateral carotid occlusion, the superior laryngeal nerves and the vagi were sectioned bilaterally in addition to the ADNs. This eliminates reflex effects of the potential activation of these sensory afferents that may mask or oppose the pressor response to the isolated carotid sinus hypotension. Possible contribution to the response by carotid chemoreceptors was also suppressed by ventilation with 100% O₂²⁸.

Supplementary Material

Refer to Web version on PubMed Central for supplementary material.

Acknowledgments

We thank Sarah Porter and Courtney Cable for assistance with word processing and manuscript preparation, Shawn Roach for help creating and editing the figures, Rubens Fazan, Jr. for assistance in analyses of data on aortic baroreceptor nerve activity, and David Dellsperger for assisting Donald Morgan in studies of electrical stimulation of the aortic depressor nerve done in the lab of Kamal Rahmouni and Allyn Mark. We also thank the University of Iowa Core DNA Facility, the central microscopy facility and the animal care facility for assistance.

SOURCES OF FUNDING

This work was supported by grant HL14388-37 from the National Institutes of Health (F.M.A. and M.W.C.), the VA Merit Review Award from the Department of Veterans Affairs (M.W.C.), the HHMI (M.J.W.), and Heartland Affiliate Postdoctoral Fellowships from the American Heart Association (R.S.).

References

1. Landgren S. On the excitation mechanism of the carotid baroreceptors. *Acta Physiol Scand* 1952;26:1–34. [PubMed: 12985395]
2. Heymans, C.; Neil, E. *Reflexogenic Areas of the Cardiovascular System*. Boston: Little, Brown & Co; 1958. p. 1-271.

3. Mortara A, et al. Arterial baroreflex modulation of heart rate in chronic heart failure. *Circulation* 1997;96:3450–3458. [PubMed: 9396441]
4. La Rovere MT, Bigger JT Jr, Marcus FI, Mortara A, Schwartz PJ. Baroreflex sensitivity and heart-rate variability in prediction of total cardiac mortality after myocardial infarction. *The Lancet* 1998;351:478–484.
5. Robinson TG, Dawson SL, Eames PJ, Panerai RB, Potter JF. Cardiac baroreceptor sensitivity predicts long-term outcome after acute ischemic stroke. *Stroke* 2003;34:705–712. [PubMed: 12624295]
6. Guharay F, Sachs F. Stretch-activated single ion channel currents in tissue-cultured embryonic chick skeletal muscle. *J Physiol* 1984;352:685–701. [PubMed: 6086918]
7. O'Hagan R, Chalfie M, Goodman MB. The MEC-4 DEG/ENaC channel of *Caenorhabditis elegans* touch receptor neurons transduces mechanical signals. *Nature Neurosci* 2005;8(1):43–50. [PubMed: 15580270]
8. Hajduczuk G, Chapleau MW, Ferlic RJ, Mao HZ, Abboud FM. Gadolinium inhibits mechano-electrical transduction in rabbit carotid baroreceptors: implication of stretch-activated channels. *J Clin Invest* 1994;94:2392–2396. [PubMed: 7527431]
9. Drummond HA, Price MP, Welsh MJ, Abboud FM. A molecular component of the arterial baroreceptor mechanotransducer. *Neuron* 1998;21:1435–41. [PubMed: 9883735]
10. Gillespie PG, Walker RG. Molecular basis of mechanosensory transduction. *Nature* 2001;413:194–202. [PubMed: 11557988]
11. Huang M, Chalfie M. Gene interactions affecting mechanosensory transduction in *Caenorhabditis elegans*. *Nature* 1994;367:467–470. [PubMed: 7509039]
12. Price MP, Snyder PM, Welsh MJ. Cloning and expression of a novel human brain Na⁺ channel. *J Biol Chem* 1996;271:7879–7882. [PubMed: 8626462]
13. Price MP, et al. The mammalian sodium channel BNC1 is required for normal touch sensation. *Nature* 2000;407:1007–1011. [PubMed: 11069180]
14. Garcia-Anoveros J, Samad TA, Zuvella-Jelaska L, Woolf CJ, Corey DP. Transport and localization of the DEG/ENaC ion channel BNaC1 alpha to peripheral mechanosensory terminals of dorsal root ganglia neurons. *J Neurosci* 2001;21:2678–2686. [PubMed: 11306621]
15. Waldmann R, Champigny G, Bassilana F, Heurteaux C, Lazdunski M. A proton-gated cation channel involved in acid sensing. *Nature* 1997;386:173–177. [PubMed: 9062189]
16. Page AJ, et al. Different contributions of ASIC channels 1a, 2, and 3 in gastrointestinal mechanosensory function. *Gut* 2005;54:1408–1415. [PubMed: 15987792]
17. Benson CJ, Xie J, Wemmie JA, Price MP, Henss JM, Welsh MJ, Snyder PM. Heteromultimers of DEG/ENaC subunits form H⁺-gated channels in mouse sensory neurons. *PNAS* 2002;99(4):2338–2343. [PubMed: 11854527]
18. Roza C, et al. Knockout of the ASIC2 channel in mice does not impair cutaneous mechanosensation, visceral mechanonociception and hearing. *J Physiol* 2004;558:659–669. [PubMed: 15169849]
19. Drew LJ, et al. Acid-sensing ion channels ASIC2 and ASIC3 do not contribute to mechanically activated currents in mammalian sensory neurones. *J Physiol* 2004;556.3:691–710. [PubMed: 14990679]
20. Butz GM, Davisson RL. Long-term telemetric measurement of cardiovascular parameters in awake mice: a physiological genomics tool. *Physiol Genomics* 2001;5:89–97. [PubMed: 11242593]
21. Bertineiri G, et al. Evaluation of baroreceptor reflex by blood pressure monitoring in unanesthetized cats. *Am J Physiol* 1988;254:H377–H383. [PubMed: 3344828]
22. Laude D, Baudrie V, Elghozi JL. Applicability of recent methods used to estimate spontaneous baroreflex sensitivity to resting mice. *Am J Physiol Regul Integr Comp Physiol* 2008;294:R142–R150. [PubMed: 17989145]
23. Cunningham JT, Wachtel RE, Abboud FM. Mechanosensitive currents in putative aortic baroreceptor neurons in vitro. *J Neurophysiol* 1995;73:2094–2098. [PubMed: 7623100]
24. Sullivan MJ, Sharma RV, Wachtel RE, Chapleau MW, Waite LJ, Bhalla RC, Abboud FM. Non-voltage-gated Ca²⁺ influx through mechanosensitive ion channels in aortic baroreceptor neurons. *Circ Res* 1997;80:861–867. [PubMed: 9168789]

25. Snitsarev V, Whiteis CA, Chapleau MW, Abboud FM. Mechano- and chemosensitivity of rat nodose neurones—selective excitatory effects of prostacyclin. *J Physiol* 2007;582.1:177–194. [PubMed: 17478531]
26. Cunningham JT, Wachtel RE, Abboud FM. Mechanical stimulation of neurites generates an inward current in putative aortic baroreceptor neurons in vitro. *Brain Res* 1997;757:149–154. [PubMed: 9200510]
27. Ma X, Abboud FM, Chapleau MW. Analysis of afferent, central, and efferent components of the baroreceptor reflex in mice. *Am J Physiol Regul Integr Comp Physiol* 2002;283:R1033–R1040. [PubMed: 12376395]
28. Iturriaga R, Alcayaga J, Zapata P. Contribution of carotid body chemoreceptors and carotid sinus baroreceptors to the ventilatory and circulatory reflexes produced by common carotid occlusion. *Acta Physiol Pharmacol Latinoam* 1988;38(1):27–48. [PubMed: 3201995]
29. Li Z, Lee HC, Bielefeldt K, Chapleau MW, Abboud FM. The prostacyclin analogue carbacyclin inhibits Ca^{2+} -activated K^{+} current in aortic baroreceptor neurones of rats. *J Physiol* 1997;501.2:275–287. [PubMed: 9192300]
30. La Rovere MT, et al. Baroreflex sensitivity and heart rate variability in the identification of patients at risk for life-threatening arrhythmias. *Circulation* 2001;101:2072–2077. [PubMed: 11319197]
31. Lawrence IG, et al. Is impaired baroreflex sensitivity a predictor or cause of sudden death in insulin-dependent diabetes mellitus? *Diabetic Medicine* 1997;14:82–85. [PubMed: 9017359]
32. Zucker IH, et al. Chronic baroreceptor activation enhances survival in dogs with pacing-induced heart failure. *Hypertension* 2007;50:904–910. [PubMed: 17846349]
33. Li M, et al. Vagal nerve stimulation markedly improves long-term Survival after chronic heart failure in rats. *Circulation* 2004;109(1):120–124. [PubMed: 14662714]
34. Epstein SE, et al. Treatment of angina pectoris by electrical stimulation of the carotid-sinus nerves. *NEJM* 1969;280:971–978. [PubMed: 4888077]
35. Filippone JD, Bisognano JD. Baroreflex stimulation in the treatment of hypertension. *Curr Opin Nephrol Hypertens* 2007;16:403–408. [PubMed: 17693753]
36. Driscoll M, Chalfie M. The mec-4 gene is a member of a family of *Caenorhabditis elegans* genes that can mutate to induce neuronal degeneration. *Nature* 1991;349:588–593. [PubMed: 1672038]
37. Huang M, Chalfie M. Gene interactions affecting mechanosensory transduction in *Caenorhabditis elegans*. *Nature* 1994;367:467–470. [PubMed: 7509039]
38. Tavernarakis N, Shreffler W, Wang SL, Driscoll M. *unc-8*, a member of the DEG/ENaC superfamily, encodes a subunit of a candidate stretch-gated motor neuron channel that modulates locomotion in *C. elegans*. *Neuron* 1997;18:107–119. [PubMed: 9010209]
39. Chalfie M, Driscoll M, Huang M. Degenerin similarities. *Nature* 1993;361:504. [PubMed: 8429902]
40. Corey DP, Garcia-Anoveros J. Mechanosensation and the DEG/ENaC ion channels. *Science* 1996;273:323–324. [PubMed: 8685718]
41. Carrattino MD, Sheng S, Kleyman TR. Epithelial Na^{+} channels are activated by laminar shear stress. *J Biol Chem* 2004;279:4120–4126. [PubMed: 14625286]
42. Awayda MS, Subramanyam M. Regulation of the epithelial Na^{+} channel by membrane tension. *J Gen Physiol* 1998;262(31):H1415–H1421.
43. Drummond HA, Gebremedhin D, Harder DR. Degenerin/epithelial Na^{+} channel proteins: components of a vascular mechanosensor. *Hypertension* 2004;44:643–648. [PubMed: 15381679]
44. Clapham DE, Montell C, Schultz G, Julius D. International Union of Pharmacology. XLIII Compendium of voltage-gated ion channels: Transient receptor potential channels. *Pharmacol Rev* 2003;55:591–596. [PubMed: 14657417]
45. O’Neil RG, Heller S. The mechanosensitive nature of TRPV channels. *Pflugers Arch* 2005;451:193–203. [PubMed: 15909178]
46. Glazebrook PA, Schilling WP, Kunze DL. TRPC channels as signal transducers. *Pflugers Arch* 2005;451:125–130. [PubMed: 15971079]
47. Desai BN, Clapham DE. TRP channels and mice deficient in TRP channels. *Pflugers Arch* 2005;451:11–18. [PubMed: 16078044]

48. Jones RCW III, Xu L, Gebhart GF. The mechanosensitivity of mouse colon afferent fibers and their sensitization of inflammatory mediators require transient receptor potential vanilloid 1 and acid-sensing ion channel 3. *J Neurosci* 2005;25:10981–10989. [PubMed: 16306411]
49. Schaefer M. Homo- and heteromeric assembly of TRP channel subunits. *Pflugers Arch* 2005;451:35–42. [PubMed: 15971080]
50. Meltzer RH, et al. Heteromeric assembly of acid-sensitive ion channel and epithelial sodium channel subunits. *J Biol Chem* 2007;282(35):25548–25559. [PubMed: 17613525]
51. Goodman MB, Schwarz EM. Transducing touch in *Caenorhabditis elegans*. *Annu Rev Physiol* 2003;65:429–452. [PubMed: 12524464]
52. Fricke B, et al. Epithelia Na⁺ channels and stomatin are expressed in rat trigeminal mechanosensory neurons. *Cell Tissue Res* 2000;266:327–334. [PubMed: 10772247]
53. Deval E, Salinas M, Baro A, Lingueglia E, Lazdunski M. ASIC2b-dependent regulation of ASIC3, an essential acid-sensing ion channel subunit in sensory neurons via the partner protein PICK-1. *J Biol Chem* 2004;279:19531–19539. [PubMed: 14976185]
54. Guo GB, Thames MD, Abboud FM. Differential baroreflex control of heart rate and vascular resistance in rabbits. *Circ Res* 1982;50(4):554–565. [PubMed: 6802513]
55. Guo GB, Abboud FM. Arterial baroreflexes in renal hypertensive rabbits. Selectivity and redundancy of baroreceptor influence on heart rate, vascular resistance, and lumbar sympathetic nerve activity. *Circ Res* 1983;53(2):223–234. [PubMed: 6883646]
56. Guo GB, Abboud FM. Impaired central mediation of the arterial baroreflex in chronic renal hypertension. *Am J Physiol* 1984;246:H720–H727. [PubMed: 6720985]
57. Wemmie JA, et al. Overexpression of acid-sensing ion channel 1a in transgenic mice increases acquired fear-related behavior. *PNAS* 2004;101:3621–3626. [PubMed: 14988500]

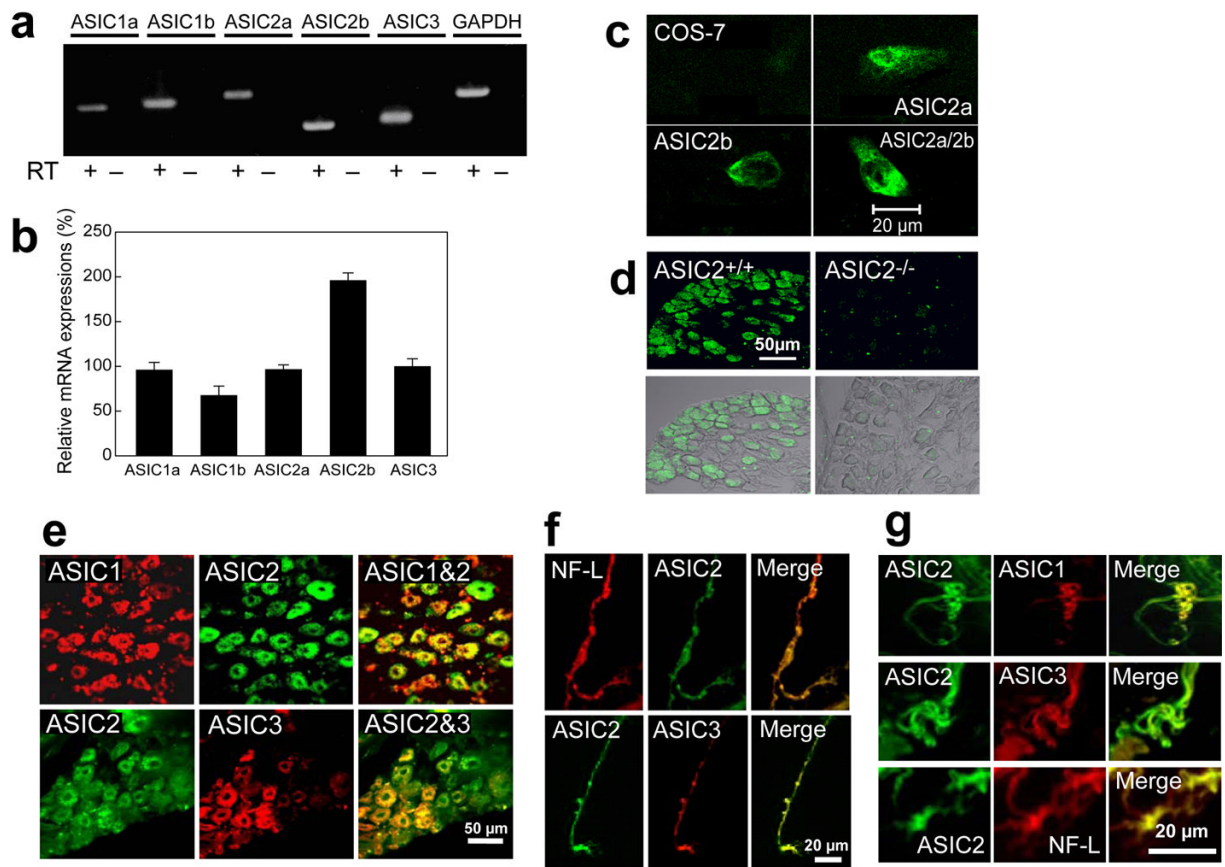


Figure 1. Expression of ASICs and their localization in mouse nodose ganglia and aortic baroreceptor terminals

a, Reverse transcription of total RNAs from nodose ganglia. All 5 isomers ASIC1a, 1b, 2a, 2b, and 3 were expressed.

b, Relative mRNA expression. Data (mean \pm s.e.m.) were obtained by combining 2 ganglia from each of 5 mice. ASIC3 expression was used as the reference. Calculation of copy numbers of target RNA products showed that ASIC2b was more prominently expressed than ASIC1a and 1b and ASIC2a and 3, ($P < 0.05$, unpaired t-test).

c, Immunolocalization of ASIC proteins in transfected COS-7 cells. COS-7 cells transfected with ASIC2a and 2b genes in plasmid fluoresced with ASIC2 antibodies (green) whereas the untransfected COS cell (upper left corner) did not.

d, Immunohistochemical staining of two nodose ganglia shows ASIC2 antibody fluorescence in the ganglion from an ASIC2^{+/+} mouse on the left, but not in the ganglion from the ASIC2^{-/-} mouse on the right. The lower images show the same ganglia in a differential interference contrast to highlight some unstained neurons in ASIC2^{+/+} on the left and the absence of stained neurons in ASIC2^{-/-} on the right.

e, Specific antibodies for ASIC1, ASIC2, and ASIC3 were used. Antibodies of ASIC1 and ASIC3 each co-localize with ASIC2 in 2 different nodose ganglia.

f, Double labeling of 2 baroreceptor nerve fibers from mouse aortic arch shows antibodies of neurofilament NF-L and ASIC3 each co-localizing with ASIC2.

g, Panels show labeled nerve terminals in the mouse aortic arch with antibodies of ASIC1, ASIC3, and neurofilament NF-L each co-localizing with ASIC2.

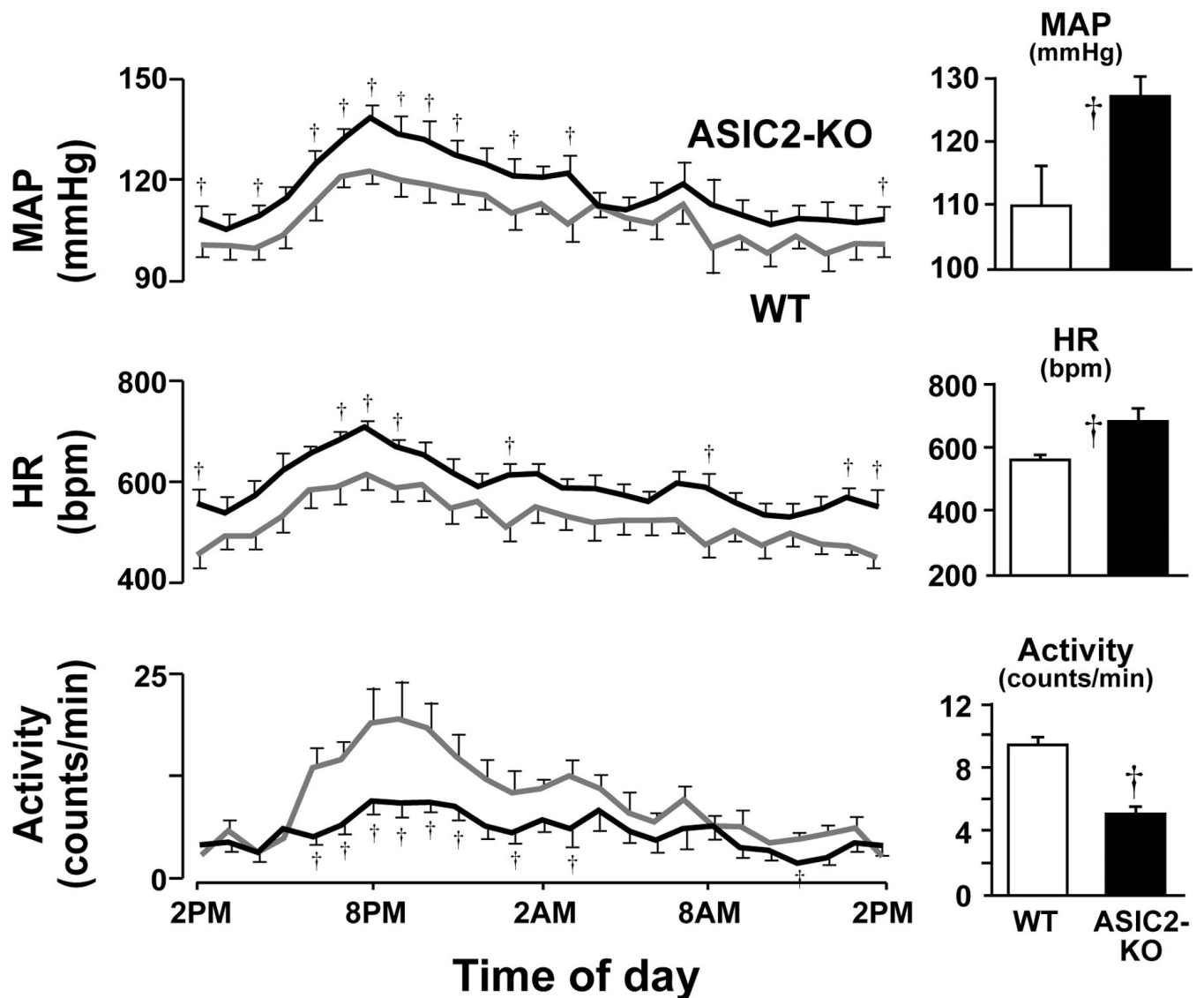


Figure 2. Continuous telemetric recordings of arterial blood pressure, heart rate and locomotor activity in conscious mice with ASIC 2 deletion and in WT mice

Continuous measurements of mean arterial pressure, heart rate, and locomotor activity over a 24 hour period are represented here by the means \pm s.e.m. of hourly values obtained from 18 ASIC2-KO and 7 WT mice. Mean arterial pressure (MAP) and heart rate (HR) were significantly higher in the null mice despite a significantly lower level of locomotor activity compared to WT mice. The differences between the 2 groups were significant ($\dagger P < 0.05$, by two-way analysis of variance ANOVA). The \dagger signs indicate significant differences at specific time points throughout the diurnal cycle as well as in the average 24-hour measurements represented in the bar graphs for MAP, HR, and locomotor activity ($P < 0.05$ ANOVA, Fisher's PLSD Post hoc).

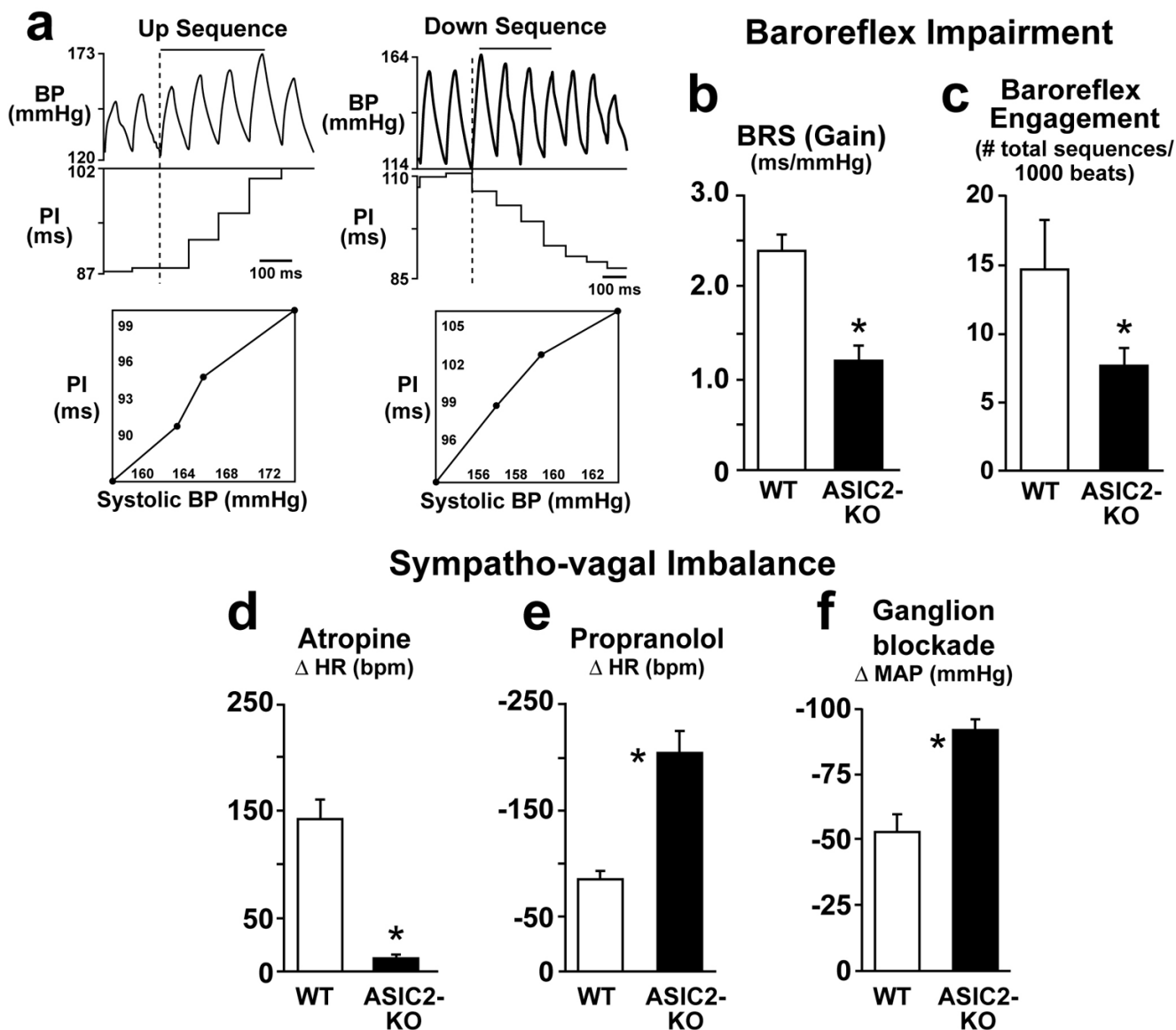


Figure 3. Baroreflex and sympatho-vagal balance in conscious mice
The baroreflex during spontaneous fluctuations in arterial pressure and heart rate is impaired in ASIC2 KO (Figures 3a, b and c).

a, The arterial pressure tracings (BP mmHg) represent examples of an Up Sequence of 4 beats when arterial pressure was rising (top left tracing) and a Down Sequence of 4 beats when arterial pressure was falling (top right tracing). The steps below the pressure tracings indicate the corresponding pulse intervals (PI ms). The graphs below the tracings represent computer generated plots of the 4 consecutive systolic pressures and their corresponding PIs which in these examples gave an r^2 value of ≥ 0.85 . Such sequences, which are referred to as baroreflex sequences, were obtained from blood pressure data sampled at 2000Hz for ~1 hour on 2 separate days between 10:00 a.m. and 3:00 p.m. The average number of sequences recorded per 1000 beats during periods of activity, and the average gain or slope of these sequences which reflects baroreflex sensitivity (BRS), were calculated for each animal. The group data are shown in Figures 3b and 3c.

b, Baroreflex sensitivity (BRS), expressed as the change in PI (ms) per change in systolic blood pressure (mmHg), was significantly reduced in the ASIC2 null mice (n=14) compared to WT (n=5) (*P<0.05).

c, The number of sequences per 1000 beats that reflect the frequency of engagement of the baroreflex during spontaneous fluctuations in arterial pressure in the awake state was significantly lower in the ASIC2-KO mice.

The sympatho-vagal balance is disrupted in ASIC2 KO (Figures 3d, e, and f).

d, the tachycardic response to atropine is suppressed in the KO mice, reflecting a very low parasympathetic tone compared to WT (HR in beats per min. increased from 513 ± 14 to 653 ± 18 i.e. $\Delta 140 \pm 18$ in WT mice, n = 9; vs. an increase from 647 ± 27 to 656 ± 26 i.e. $\Delta 8 \pm 2$ in KO mice, n = 8).

e, the bradycardic response to propranolol (Δ HR in bpm) was greater in ASIC2 KO (from 687 ± 23 to 485 ± 8 i.e. $\Delta -202 \pm 20$, n=8) vs. WT mice (from 558 ± 31 to 477 ± 24 i.e. $\Delta -80 \pm 15$, n=9) reflecting an increased sympathetic tone in the null mice.

f, the resting mean arterial pressure was 120 ± 5 mmHg in WT (n=4) and 128 ± 9 mmHg ASIC2 KO mice (n=5). The fall in mean arterial pressure (MAP) with ganglion blockade with chlorisondamine was greater in the KO vs. WT mice reflecting predominantly a significant increase in the neurogenic sympathetic control of vascular resistance in ASIC2-KO.

(*asterisks indicate significant differences between the 2 groups, P<0.05 by unpaired t-test)

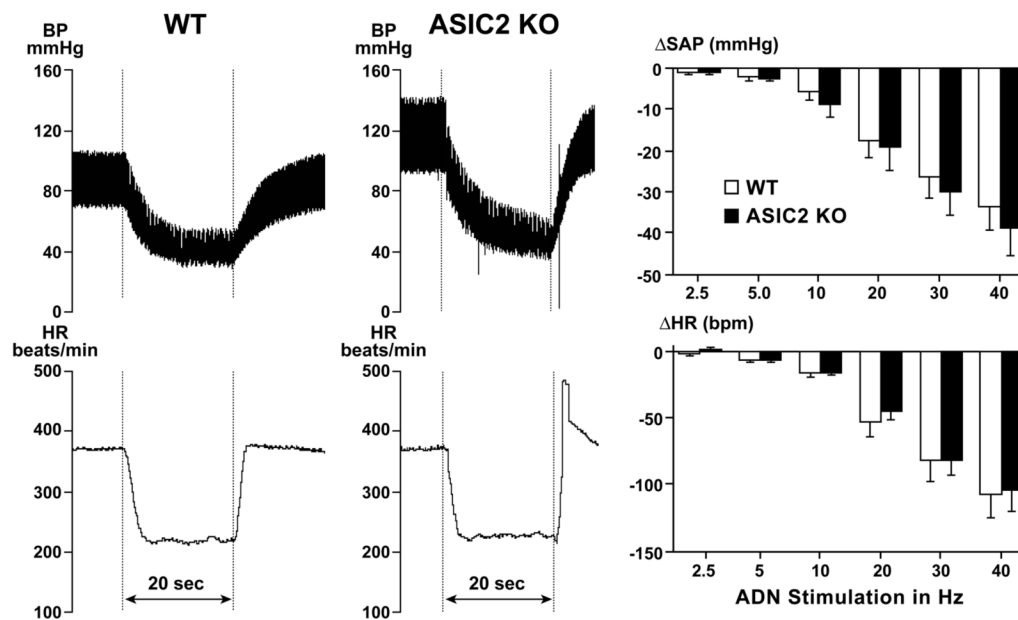


Figure 4. Responses to electrical stimulation of the aortic depressor nerve in anesthetized mice
 The tracings represent rapid and transient decreases in arterial blood pressure (BP mmHg) and heart rate (HR beats per min.) during a 20 sec. period (horizontal bar) of electrical stimulation with pulses of 2 msec. at 40 Hz and 10 V in a WT mouse (left panels) and an ASIC2 KO mouse (right panels). Bar graphs show the group data (mean \pm SE) from WT (open bars, n=7) and ASIC2 KO (black bars, n=9) which indicate that responses to graded frequencies of stimulation from 2.5 to 40 Hz were not statistically different in the 2 groups (ANOVA—group comparison by Student-Newman-Keuls test, $P=0.60$ and 0.77 for systolic arterial pressure (SAP) and heart rate respectively).

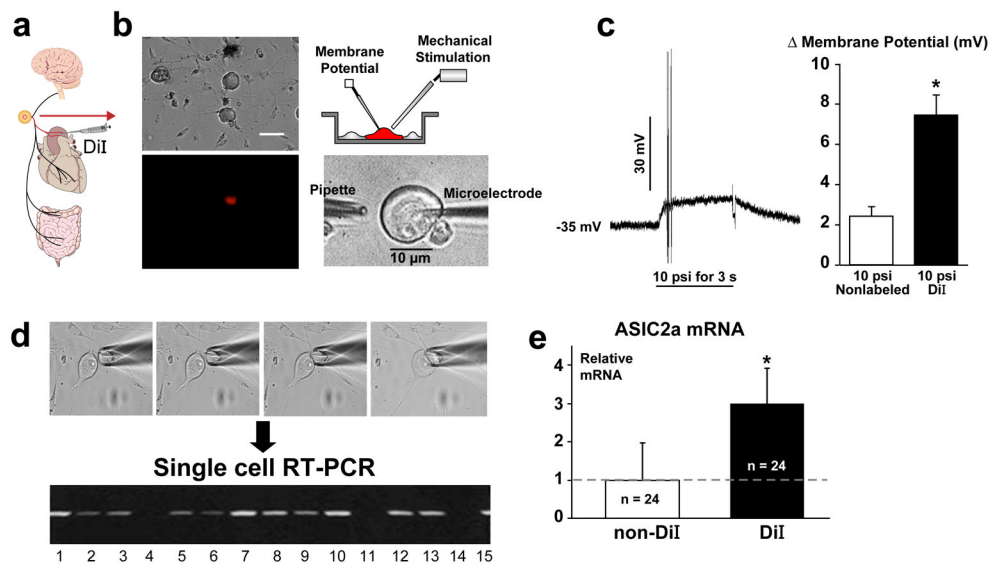


Figure 5. Mechanically-induced depolarization and ASIC2 mRNA expression in aortic vs. non-aortic nodose neurons

a, Schematic of different sensory afferents to nodose ganglia showing injection of the tracer DiI into the aortic arch adventitia to label selectively aortic baroreceptor neurons in the nodose ganglia.

b, Dispersed nodose neurons in culture show one fluorescent DiI labeled aortic baroreceptor neuron and several non-labeled ones.

c, The mechanical stimulus initiated a rapid depolarization which triggered transient action potential discharge in a DiI labeled mouse neuron. The sharp brief negative deflection at the end of the sustained depolarization represents the response to injection of a transient hyperpolarizing current given to measure changes in membrane conductance. The bar graph shows that labeled aortic baroreceptor neurons from 12 mice depolarized much more ($n=35$, 7.45 ± 1.03 mV) than non-labeled nodose neurons from 18 mice ($n=45$, 2.42 ± 0.51 mV) ($*P < 0.05$, unpaired t-test). These depolarizations were from their resting membrane potentials. Membrane conductances measured in DiI positive cells averaged 7.67 ± 0.70 nS before mechanical stimulation and increased during stimulation to 9.06 ± 0.88 nS ($P < 0.005$, $n=19$). Corresponding values in non DiI cells were 13.26 ± 1.03 and 13.15 ± 1.07 respectively ($P=0.76$, $n=20$). From a holding membrane potential of -60 mV, achieved by current injections, the differences in mechanically-induced depolarizations were greater with corresponding values of 8.72 ± 1.83 mV and 1.57 ± 0.57 mV respectively.

d, Single cell RT-PCR of ASIC2a mRNA reveals varying expression levels in 15 individual rat nodose neurons in culture. In different neuron populations studied, ASIC2a was expressed in 55 to 80% of the cells.

e, Normalization using housekeeping gene GAPDH revealed that DiI labeled rat aortic baroreceptor neurons had significantly higher ASIC2a mRNA levels compared to non-DiI neurons ($*P < 0.05$, unpaired t-test).

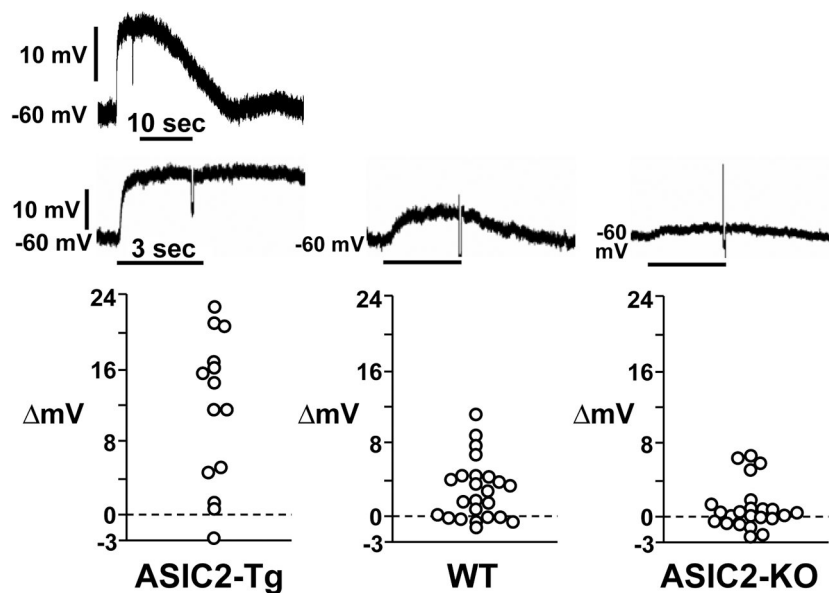


Figure 6. Mechanosensitivity of mouse nodose neurons is significantly reduced in ASIC2 null vs WT and Tg

Responses to 3 sec. mechanical stimulations of nodose neurons from WT (n=24), ASIC2 -KO (n=23) and ASIC2 transgenic (Tg) (n=14) mice. The tracings above each graph are depolarizations of a mechanosensitive neuron selected from each group. The tracing from the Tg neuron is portrayed at different time scales to show the delayed recovery from depolarization. A holding membrane potential was set at -60 mV in all neurons to minimize differences in responses caused by variations in resting membrane potentials. The number of neurons that depolarized less than 1mV or hyperpolarized with mechanical stimulation was significantly greater (chi-test $P < 0.001$) in the null mice (17 of 23) than in the WT (9 of 24). Only one neuron of 14 in the Tg group hyperpolarized. The difference between groups was highly significant by ANOVA (F value of 22.64 vs. Fcrit of 3.15). The neurons from ASIC2 Tg mice had a significantly greater depolarization (11.24 ± 2.20 mV) than seen in WT (2.73 ± 0.67 mV) or in ASIC2 null mice (0.86 ± 0.53 mV) ($P < 0.01$ and < 0.05 respectively: ANOVA, Post Hoc). Also the response in WT was significantly greater than in KO mice (Wilcoxon Rank Sum, $P = 0.046$; unpaired t-test 2 tail $P = 0.035$; 1 tail $P = 0.017$).

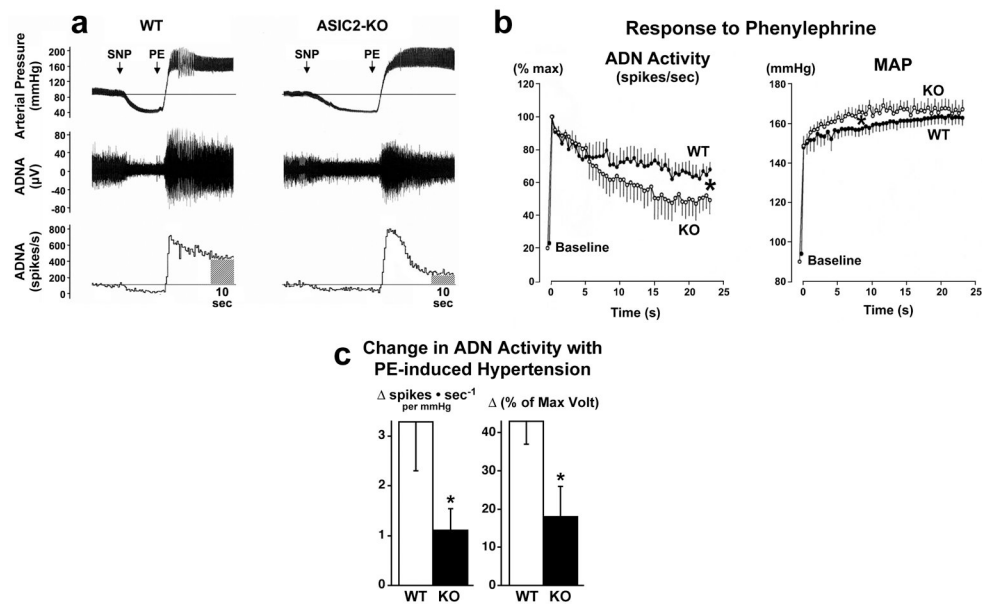


Figure 7. Aortic depressor nerve activity is reduced in ASIC2 null mice

a, The tracings show phasic arterial pressure and aortic depressor nerve activity (ADNA) in a WT and an ASIC2 -KO mouse. ADNA is shown as the magnitude of voltage of action potentials in μ V (middle tracings) and as number of spikes generated per second (lower tracings) during changes in arterial pressure with sodium nitroprusside injections (SNP) and phenylephrine injections (PE). Although the peak level of nerve activity during the onset of the pressor response to PE was comparable in both groups, the activity was not maintained in ASIC2 KO and declined rapidly reaching a significantly lower level than in WT. The WT record shows a transient reflex bradycardia apparent following the peak rise in pressure after which both pressure and nerve activity stabilized. Comparisons were made of recordings of both BP and ADNA obtained in the control state before the injection of SNP, and in the steady state during the period between 15 and 25 seconds following the maximum increase in ADNA with injection of PE.

b, The left graph represents data points obtained every 500 msec after the maximum increase in spike frequency with PE, and expressed as a % of the peak frequency (% max). The right graph shows the corresponding mean arterial pressure (MAP) over the period of 25 seconds following PE injections. The values are means \pm s.e.m. obtained from ASIC2 -KO mice ($n=6$) and WT mice ($n=7$). The ADN activity declined rapidly in KO mice to levels that were significantly lower than in WT ($*P<0.001$ by ANOVA; Newman-Keuls Test). Conversely, MAP rose to statistically higher levels in KO mice initially ($*P<0.001$ by ANOVA; Newman-Keuls Test) during the first 10 seconds and then plateaued to levels comparable to those in WT.

c, The bars represent increases in ADN activity in WT and ASIC2 KO from baseline control values (integrated over a 10-second period prior to SNP injection) to the values obtained during a 10-second period of sustained increase in pressure between 15 and 25 sec. after PE when MAP was not statistically different between the 2 genotypes. The left bars are the increases in spikes \cdot sec⁻¹ for every mmHg increase in pressure from control to the sustained plateau level. The right bars represent the differences in integrated voltage between baseline and plateau levels both expressed as % of max. voltage. The responses in null mice were less than half those seen in WT mice ($*P<0.05$ unpaired t-test).

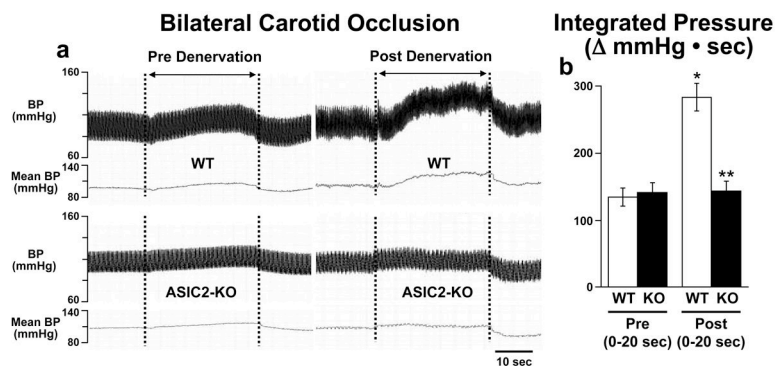


Figure 8. Responses to bilateral carotid occlusion before and after section of the ADNs show enhancement of the pressor response with denervation in WT but not in ASIC2 -KO mice

a, Tracings represent increases in phasic (BP) and mean arterial pressure (mean BP) in mmHg during periods of bilateral carotid occlusion for 30 seconds (between the vertical dotted lines) in two anesthetized mice on 100% oxygen. One record was from a WT mouse (top) and the other from an ASIC2 -KO (bottom). Before ADN section (Pre Denervation) the pressor responses were comparable in WT and null mice (left tracings) whereas after ADN section (Post Denervation) the pressor responses were significantly enhanced in the WT but not in the KO (right tracings).

b, The bar graphs contrast the mean \pm SE of the integrated increase in pressure over time from 0 to 20 sec of carotid occlusion (Δ mmHg \cdot sec) in WT (open bars, n=6) vs. KO mice (black bars, n=6). Pre and Post responses were those obtained before and after section of the ADNs. ADN section caused a significant increase in the pressor response in the WT (* P <0.02) but not in the KO. Following ADN section (Post 0–20sec), the pressor response was significantly less in the ASIC2 null mice than in WT (** P =0.006).